Near–field optical transmittance of metal particle chain waveguides

Christian Girard[1] **and Romain Quidant**[2]

[1] *CEMES, UPR-CNRS 8011, 29 rue Jeanne Marvig, 31055 Toulouse, France*
[2]*ICFO–Institut de Ciències Fotòniques, c/ Jordi Girona 29, Nexus II, 08034 Barcelona, Spain*

Abstract: A self–consistent model based on the classical field-susceptibilities formalism has been developed to simulate recent experiments where metallic particle chain waveguides are addressed locally by the tip of a Scanning Near-Field Optical Microscope (SNOM) [1]. This approach which accounts for the actual optical response of the particles leads to a reliable description of both near-field transmittances and losses of this kind of integrated devices.

OCIS codes: (180.5810) Scanning Microscopy, (240.5420) Polaritons, (260.3910) Metals optics of, (350.3950) Micro-optics

References and links

1. S. A. Maier, P. G. Kik, H. A. Atwater, S. Meltzer, E. Harel, B. E. Koel, and A. A. G. Requicha, "Local detection of electromagnetic energy transport below the diffraction limit inmetal nanoparticle plasmon waveguides," Nature Materials **2**, 229 (2003).
2. W. L. Barnes, A. Dereux, and T. W. Ebbesen, "Surface Plasmon subwavelength optics," Nature **424**, 824 (2003).
3. J. R. Krenn, J. C. Weeber, E. Bourillot, J. P. Goudonnet, B. Schider, A. Leitner, F. R. Aussenegg, and Ch. Girard, "Squeezing the optical near-field zone by plasmon coupling of metallic nanoparticles," Phys. Rev. Lett. **82**, 2590 (1999).
4. S. A. Maier, M. L. Brongersma, P. G. Kik, and H. A. Atwater, " Observation of near-field coupling in metal nanoparticle chains using far-field polarization spectroscopy," Phys. Rev. B **65**, 193408 (2002).
5. M. L. Brongersma, J. W. Hartman, and H. A. Atwater, "Electromagnetic energy transfer and switching in nanoparticle chain arrays below the diffraction limit," Phys. Rev. B **62**, R16356 (2000).
6. M. Quinten, A. Leitner, J. R. Krenn, and F. R. Aussenegg, "Electromagnetic energy transport via linear chains of silver nanoparticles," Opt. Lett. **23**, 1331 (1998).
7. S. A. Maier, P. G. Kik, and H. A. Atwater, "Optical pulse propagation in metal nanoparticle chain waveguides," Phys. Rev. B **67**, 205402 (2003).
8. C. Girard, A. Dereux and C. Joachim, "Resonant optical tunnel effect through dielectric structures of subwavelength cross-sections," Phys. Rev. E **59** 6097 (1999)
9. R. Quidant, J. C. Weeber, A. Dereux, D. Peyrade, C. Girard and Y. Chen, "Spatially resolved energy transfer through mesoscopic heterowires," Phys. Rev. E **65** 036616 (2002).
10. H. J. Maas *et al.*, "Imaging of photonic nanopatterns by scanning near-field optical microscope," J. Opt. Soc. Am. B **19**, 1295 (2002).
11. M. Brun, A. Drezet, H. Mariette, N. Chevalier, J. C. Woehl, and S. , "Remote optical addressing of single nano-objects," Europhys Lett. **64**, 634 (2003).
12. C. Girard and X. Bouju, "Coupled electromagnetic modes between a corrugated surface and a thin probe tip," J. Chem. Phys. **95**, 2056 (1991).
13. O. J. F. Martin, C. Girard, and A. Dereux, "Generalized field propagator for electromagnetic scattering and light confinement," Phys. Rev. Lett. **74**, 526 (1995).
14. E. D. Palik, *Handbook of Optical Constants of Solids* (Academic, San Diego, CA, 1985).
15. G. Colas des Francs and C. Girard, "Coplanar devices for optical addressing of single molecules", Nanotechnology **12**, 75 (2001).

#5341 - $15.00 US Received 21 September 2004; revised 16 November 2004; accepted 25 November 2004

1. Introduction

The optical addressing of subwavelength volumes represents one of the major challenges for the future of integrated optical devices. Among many others strategies, optical devices involving surface plasmon polaritons sustained by metallic nanostructures (the so–called plasmonics) are currently being investigated [2]. An interesting class of experimental studies based on plasmonic excitations, exploits ensembles of metallic nanoparticles (chains, arrays, ...) [3, 4, 5]. In this kind of system, each individual nanostructure rounds up the electron gas in the three dimensions and gives rise to "Localized Surface Plasmons"(LSPs). These resonances are associated with a significant increase of both absorption and scattering phenomena and with an enhancement of their local field. Within an ensemble of closely packed particles, the coupling implies essentially the evanescent fields that tails off each individual particles (evanescent coupling). Calculations performed by Quinten *et al* [6] have shown that this kind of interaction could be optimized to promote the transfer of visible light through linear chains of silver nanoparticles with diameters typically scaled down to 30 *nm*. Very recently direct experimental evidence of this kind of short range coupling has been reported [1] by measuring the electromagnetic energy transport along silver nanoparticle plasmon waveguides. From a numerical point of view, the study of such complex optical systems is rather challenging regarding the computational difficulties associated with both the geometry and the important role played by the evanescent states. For example, the difficulties due to the exponential behavior of the evanescent waves limit the applicability of the boundary-condition based methods. Recently, it has been shown that a chain of closely packed noble metal particles with 50 *nm* diameter can be modeled by a chain of coupled dipoles. Within the simple framework of the dipolar approximation, the dispersion relation of the chain can be easily derived, allowing the energy of both longitudinal and transversal modes to be compared [5]. However, for larger and non–spherical particles lithographicallly designed at the surface of a sample, the point–like description becomes questionable and more elaborated models are highly desirable. Although the Finite Difference Time Domain (FDTD) method supplies precious information in a fast pulsed–regime [7], it suffers from limitations for reproducing a permanent illumination regime and thus for computing the transmittance of this kind of systems, and to predict consequently their guiding abilities [8]. For these different reasons, we describe in this paper new numerical data obtained in the vicinity of metallic chains by adapting and extending the formalism of classical field–susceptibilities previously developed for Near Field Optics (NFO). Access to different quantities of interest, i. e. field maps and optical transmittances, is made easier by applying this technique.

2. Theoretical background

2.1. Geometry

When describing the propagation of light in ordered or partially ordered mesoscopic material structures (thus breaking the homogeneity condition) both the radiative and evanescent components of the electromagnetic field must be accounted for. For a given band of frequencies, the decay range of evanescent waves may be commensurate with the material structure or with parts of it. In this case, high values of the transmission coefficient of the electromagnetic energy can be expected. In other words, the overlap of evanescent components generated by two material structures or defects establish the physical link that can open new optical channels. As it may be intuitively understood, such periodic or pseudo–periodic materials modulate drastically the amount of transferred energy as a function of the incident frequency. For example, it was demonstrated both theoretically and experimentally that the introduction of a suitable periodic alignment of mesoscopic dielectric pads allows for the opening of transparent windows within a quasi-optical band-gap [8, 9]. In this study, we consider the system described in Fig. 1 where a

#5341 - $15.00 US Received 21 September 2004; revised 16 November 2004; accepted 25 November 2004

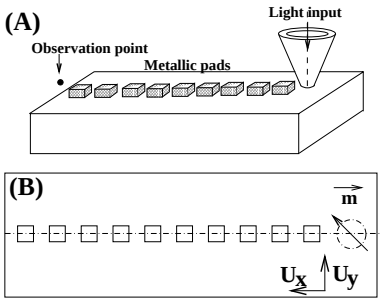

Fig. 1. (A) Perspective view of a periodic and linear chain of metal particles optically addressed by the extremity of a SNOM tip. (B) Top view of the cartesian frame we used to perform the numerical simulations. The arrow inside the dashed circle schematizes the SNOM tip dipole and the (OZ) axis is perpendicular to the figure.

linear chain of gold pads (100 *nm* side square basis and 40 *nm* height) lies onto a glass substrate. The spacing distance between each particle is fixed at 100 *nm*. These parameters, that match the one of the fabricated system of reference [3], have been chosen as they can be achieved with good reproducibility by conventional e-beam lithography. We will assume that one of the chain extremities is optically excited with the tip of a scanning near–field optical microscope (SNOM).

2.2. Illumination field $\mathscr{E}_0(\mathbf{r},t)$

Several studies [10, 11] indicate that a SNOM behaves like a quasi–pointlike dipolar light source $\mathbf{m}(t)$ oscillating in the plane parallel to the surface of the sample (XOY) plane in Fig. 1(B). Consequently, such probes represent also a versatile tool for the optical addressing at the nanometer scale [1, 11]. We will assume that the effective tip dipole $\mathbf{m}(t)$ is driven by an external monochromatic excitation of angular frequency ω_0 and polarized in a direction $\mathbf{u}$ parallel to the surface so that:

$$\mathbf{m}(t) = \mathbf{u} m \cos(\omega_0 t) \; . \tag{1}$$

In the absence of any nanostructure above the transparent sample, the zeroth order electric field $\mathscr{E}_0(\mathbf{r},t)$ generated by the SNOM tip is given by

$$\mathscr{E}_0(\mathbf{r},t) = \int \mathscr{E}_0(\mathbf{r},\omega) \exp(-i\omega t) d\omega \; , \tag{2}$$

with

$$\mathscr{E}_0(\mathbf{r},\omega_0) = \mathbf{S}(\mathbf{r},\mathbf{r}_{tip},\omega) \cdot \mathbf{m}(\omega) \; , \tag{3}$$

where, $\mathbf{r}_{tip}$ is the tip position, $\mathbf{m}(\omega)$ is the Fourier transform of the oscillating tip dipole, and $\mathbf{S}(\mathbf{r},\mathbf{r}_{tip},\omega)$ represents the field–susceptibility of the bare surface. This dyadic tensor can be split into two well–identified contributions $\mathbf{S}^0$ and $\mathbf{S}^{surf}$ that describe, respectively, free space propagation and surface reflection. In a cartesian frame (xyz), the nine (α,β) components of these two tensors are well known. Those associated with $\mathbf{S}^0$ are analytical

$$\mathbf{S}^0_{\alpha,\beta}(\mathbf{r},\mathbf{r}_{tip},\omega) = A_{\alpha,\beta} \exp(ik_0 R) \; , \tag{4}$$

with

$$A_{\alpha,\beta} = \left\{ -\frac{k_0^2}{R^3}(R_\alpha R_\beta - R^2\delta_{\alpha,\beta}) + (\frac{1}{R^5} - \frac{ik_0}{R^4})(3R_\alpha R_\beta - R^2\delta_{\alpha,\beta}) \right\} \; , \tag{5}$$

#5341 - $15.00 US Received 21 September 2004; revised 16 November 2004; accepted 25 November 2004

where $k_0 = \omega_0/c$ is the wave vector in vacuum, and $\mathbf{R} = \mathbf{r} - \mathbf{r}_{tip}$. The calculation of the surface contribution components involves a two–dimensional integral over the surface wave vector $\mathbf{k}_{\|} = (k_x, k_y)$. The calculation is given in reference [12].

2.3. Electric near–field $\mathscr{E}(\mathbf{r},t)$ transmitted along the chain

From the knowledge of the Fourier Transform $\mathscr{E}_0(\mathbf{r},\omega)$ (cf. Eqs. 3) of the SNOM illumination field, it is possible to describe the electric near–field $\mathscr{E}(\mathbf{r},t)$ everywhere in the system by performing an integration over the volume *v* occupied by the metal particles

$$\mathscr{E}(\mathbf{r},t) = \int \exp(-i\omega t)dt \int_v d\mathbf{r}' \mathscr{K}(\mathbf{r},\mathbf{r}',\omega)\cdot\mathscr{E}_0(\mathbf{r}',\omega)\ , \tag{6}$$

where, as described in reference [13], $\mathscr{K}(\mathbf{r},\mathbf{r}',\omega)$ represents a *generalized propagator* associated with the isolated system. This dyadic tensor is given by

$$\mathscr{K}(\mathbf{r},\mathbf{r}',\omega) = \mathscr{I}\,\delta(\mathbf{r}-\mathbf{r}') + \mathscr{S}(\mathbf{r},\mathbf{r}',\omega)\cdot\chi(\omega)\ , \tag{7}$$

where $\mathscr{I}$, $\mathscr{S}$, and χ are respectively the unity tensor, the field susceptibility of the entire system, and the optical response of the metal that composes the nanostructures. To compute the field susceptibility tensor $\mathscr{S}$ required to obtain the *generalized propagator*, we use Dyson's equation

$$\begin{aligned}\mathscr{S}(\mathbf{r},\mathbf{r}',\omega) &= \mathbf{S}^0(\mathbf{r},\mathbf{r}',\omega) + \mathbf{S}^{surf}(\mathbf{r},\mathbf{r}',\omega) \\ &+ \int_v d\mathbf{r}''[\mathbf{S}^0(\mathbf{r},\mathbf{r}'',\omega) + \mathbf{S}^{surf}(\mathbf{r},\mathbf{r}'',\omega)]\cdot\chi(\omega)\cdot\mathscr{S}(\mathbf{r}'',\mathbf{r}',\omega)\ ,\end{aligned} \tag{8}$$

that can be solved by using the numerical algorithm described in [13]. After replacing equation (3) into equation (6), we can write the components of the local electric field

$$\mathscr{E}_\alpha(\mathbf{r},t) = E_\alpha(\mathbf{r},\omega_0)\cos(\omega_0 t + \Phi_\alpha(\mathbf{r},\omega_0))\ , \tag{9}$$

where the amplitude is given by

$$\begin{aligned}E_\alpha(\mathbf{r},\omega_0) = m\{&\Re^2\Big(\int_v d\mathbf{r}'\mathscr{K}_{\alpha,\beta}(\mathbf{r},\mathbf{r}',-\omega_0)\mathbf{S}_{\beta,\gamma}(\mathbf{r}',\mathbf{r}_{tip},-\omega_0)\Big)u_\gamma \\ &+\Im^2\Big(\int_v d\mathbf{r}'\mathscr{K}_{\alpha,\beta}(\mathbf{r},\mathbf{r}',-\omega_0)\mathbf{S}_{\beta,\gamma}(\mathbf{r}',\mathbf{r}_{tip},-\omega_0)\Big)u_\gamma\}^{1/2}\ ,\end{aligned} \tag{10}$$

and the phase by

$$\Phi_\alpha(\mathbf{r},\omega_0) = \arctan\left\{\frac{\Im\big(\int_v d\mathbf{r}'\mathscr{K}_{\alpha,\beta}(\mathbf{r},\mathbf{r}',-\omega_0)\mathbf{S}_{\beta,\gamma}(\mathbf{r}',\mathbf{r}_{tip},-\omega_0)u_\gamma\big)}{\Re\big(\int_v d\mathbf{r}'\mathscr{K}_{\alpha,\beta}(\mathbf{r},\mathbf{r}',-\omega_0)\mathbf{S}_{\beta,\gamma}(\mathbf{r}',\mathbf{r}_{tip},-\omega_0)u_\gamma\big)}\right\}\ . \tag{11}$$

Finally, the near–field intensity around the device is given by the time average of the square modulus of equation (9)

$$Int(\mathbf{r},\omega_0) = \frac{1}{2}|\mathbf{E}(\mathbf{r},\omega_0)|^2\ . \tag{12}$$

3. Numerical results

When a SNOM probe optically addresses the extremity of a chain of metal particles, the evanescent electric field that tails off the tip couples with the closest metal pad so that significant energy transfer is triggered along the chain. The transmittance of the device can be numerically analyzed by computing the near–field intensity $Int(\mathbf{r},\omega_0)$ (cf. Eq. (12)) at the line exit versus the excitation wavelength $\lambda_0 = 2\pi c/\omega_0$. For the dielectric constant of gold chains, we have

#5341 - $15.00 US Received 21 September 2004; revised 16 November 2004; accepted 25 November 2004

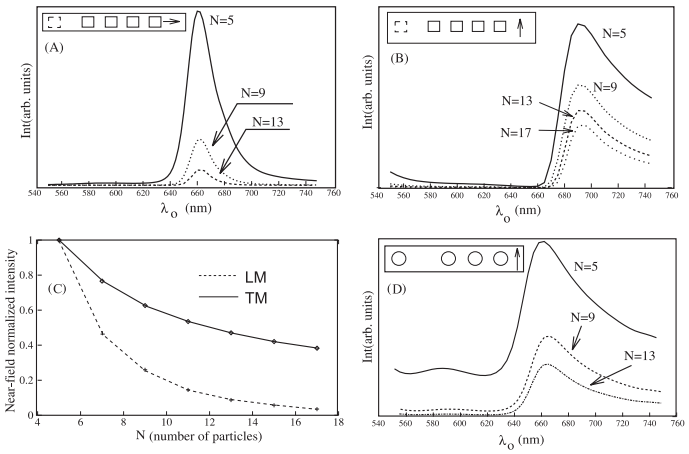

Fig. 2. (A-B) Transmittance of metal particle chains computed by increasing the number N of particles. The arrow inside the inset frame schematizes the SNOM tip dipole. (A) The tip dipole is along the longitudinal axis (LM); (B) The tip dipole is perpendicular to the chain (TM). (C) Decay of the near-field intensity at the exit of particle chain wave guides versus the number of gold pads. The intensities computed at the resonance have been normalized with respect to the intensity computed at the exit of a five particles linear chain. (D) same as (B) but with truncated cylinders of same height (40 nm) and 100 nm in diameter.

used the numerical data as tabulated by Palik [14]. In Fig. 2, the evolution of the gold chain near-field transmittance spectra as a function of the number *N* of particles is plotted for two different incident polarization states. Each curve displays a single transmission peak resulting from the coupling of the localized plasmon modes sustained by each gold pad (located around 620 *nm* for an isolated gold pad). The highest transmitted energy critically depends on the light polarization used to address the chain extremity. When the tip dipole is aligned along the chain axis (Longitudinal mode (LM)) (Fig. 2(A)), the peak is blue–shifted by 35 *nm* with respect to the case where the illuminating dipole is perpendicular to the chain (Transverse mode (TM)) (Fig. 2(B)). As mentioned in reference [7], when placing a dipolar source field at the chain extremity, the **k** wave vector is colinear to the alignment, and we explore the end of the dispersion curve where the splitting energy $\Delta E = E_T - E_L$ is negative. Figure 2(C) allows for a direct comparison of the transmission efficiency of the two modes. For the LM mode, the near–field transmitted along the chain drops down rapidly when increasing the structure length. This dramatic near–field decay is mainly due to the absence of any far–field radiation along the chain as the tip dipole is parallel to this axis. A better transfer efficiency is observed in the TM mode. In this case, all the local fields inside the metal particles oscillate coherently in directions perpendicular to the chain, and the tip dipole radiation pattern aligns along the propagation direction (OX). Consequently, for a precise wavelength range, corresponding to favorable phase shifts, the conjunction of these two effects tends to increase the transmittance of the device. Note that identical calculations on chains of truncated cylinders (Fig. 2(D)) show a more rapid decreasing of the plasmon peak versus the number of particles resulting from the reduction of the coupled surface area.

The resonant electronic tunnel effect observed in various contexts of solid state physics (superlatices, quantum wells, localized defects in metal oxide metal junctions, ...) is always accompanied by a localization of the electronic wavefunction in the tunnel barrier. In plasmonics, a similar localization phenomenon is expected. However, in the configuration analyzed in this paper, both radiative and nonradiative losses induced by scattering and energy dissipation

#5341 - $15.00 US Received 21 September 2004; revised 16 November 2004; accepted 25 November 2004

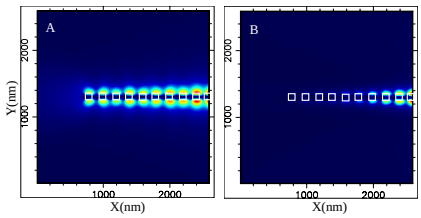

Fig. 3. Near–field optical images of a gold particle chain wave guide calculated for two different excitation wavelengths (N=17). The SNOM tip is polarized along the *OY* axis (TM). (A) λ_0 = 692 nm; (B) λ_0 = 670 nm.

along the wire, will limit the amplitude of this phenomenon. To close our numerical analysis, we present in Fig. 3, the electric field intensity maps $Int(\mathbf{r}, \omega_0)$ computed for two incident wavelengths $\lambda = 692$ nm and $\lambda = 670$ nm. In the vicinity of the transmittance resonance (cf. Fig. 2(B)), the map calculated in the case of a transverse polarization (TM) reveals the perfect commensurability existing between the variations of the field intensity along the chain and the positions of the metal edges. Regular near–field features, displaying lobes along the lateral faces of the posts, are clearly visible. The profile of the field intensity decay along these lobes provides transmission losses of about 1.5 $dB/\mu m$. This value is significantly lower compared to the results from the coupled dipole model in reference [5] ($3dB/500\ nm$). Independently of the stronger coupling between square particles, such a difference may result from the narrow meshing of the gold nanostructures (147 discretization cells per particle) that allows from a proper description of the involved proximity effects. Consequently, the realistic treatment of this effect leads to a more important red–shift of the transmission band, and locates it in an optical range where the dielectric losses of gold are weaker. Further discrepancies with the experiments from [1] may arise from other factors as the irregularities in the particles shape and separation distances. Outside of the resonance frequency range (cf. Fig. 3(B)), the spatial commensurability between the near–field intensity and the metal chain degrades and thus leads to a very low energy transfer.

4. Conclusion

We have presented a theoretical analysis of the transport of optical energy along narrow chains of metal particles. Under permanent and localized illumination, we have pointed out a transmission band where the optical near–field becomes commensurable with the metal arrangement. Transverse modes are found to lead to a higher transmittance than longitudinal modes. In spite of significant losses (scattering and electron dissipations), such structures could be good candidates for the near–field optical addressing of single molecules in coplanar geometry [15].

Acknowledgments

This work was supported in part by the European Network of Excellence (NoE) *Plasmo-Nano-Devices* (contract number 507879) and by the Spanish Ministry of Science and Technology (grant TIC2003-01038).

#5341 - $15.00 US Received 21 September 2004; revised 16 November 2004; accepted 25 November 2004